



## DESIGN OF COMBINE LOAD FREQUENCY AND VOLTAGE CONTROL OF POWER SYSTEM USING OPTIMISATION ALGORITHM

<sup>1</sup>Alimi Teslim Adekunle, <sup>2</sup>Akanbi Ibrahim Ishola and <sup>3</sup>Ajetunmobi Emmanuel Olurotimi

<sup>1</sup>Department of Electrical and Electronic Engineering, Federal Polytechnic Bida, Niger State, Nigeria

<sup>2</sup>Department of Robotics and Automation, Me2U Laboratories, Lagos State, Nigeria

<sup>3</sup>Department of Electrical and Electronics Engineering, Osun State Polytechnic Iree, Osun State, Nigeria

### ABSTRACT

Engineers' main concern is the stability of nominal frequency and voltage levels in an electric power system. If these two characteristics deteriorate, the performance and life expectancy of the power system's related equipment would suffer. Because of this, control devices must be set up and installed specifically for a given working environment to maintain the frequency and terminal voltage magnitude within acceptable ranges. An effort has been made to develop a fractional-order PID (FOPID) controller for combined frequency and voltage control issues, since the system performance may be enhanced by choosing an appropriate controller. Utilizing the moth flame optimization method, this study examines the plan and execution of the FOPID controller for simultaneous load frequency and voltage management of the power system. An AVR-based excitation voltage control system is used in the first portion of the study to illustrate the suggested method for frequency stabilization of isolated power systems. Comparison of dynamic responsiveness of the system with PID controllers improved by other intelligent methods reveals the superiority and efficacy of the suggested methodology. Also included in this project are multi-unit two-area power systems. The algorithm's capacity to be tuned is examined in great detail and compared to other algorithms.

Keywords: Automatic voltage regulator, Fractional-order control, Load frequency control, Moth flame optimization, Multi-unit multi-area system

### 1.0 Introduction

Practiced engineers' main control concern is the stability of a system's nominal frequency and voltage level (Beaufays F, Abdel-Magid Y, Widrow B (2019).). They have an impact on the performance and lifespan of any power system equipment that is connected with them. (Elgerd I (2018))To maintain the frequency and terminal voltage within the permitted limits, power system controllers are installed and configured for a particular working environment and are designed to

handle minor changes in load demands. ( Elgerd OI, Fosha C (2019)) For each generator, two loops are given. It controls actual power and frequency, whereas the automated voltage regulator (AVR) regulates reactive power and voltage magnitude. Ismail A (2020) Researchers have studied the LFC and AVR loop separately in the past. Kumar P, Kothari DP (2016) In part because of this, transients in the excitation system settle down fast and have no effect on LFC dynamics since prime mover time constant is considerably greater than excitation system time constant. Fosha CE, Elgerd OI (2019) However, the two loops do not communicate in the truest sense. Variations in frequency and voltage result from changes in the end-user's Real power is determined by the magnitude of generator voltage, which is influenced by the control action in AVR loop. Recently, academics have been concentrating on the combined LFC-AVR control issue, which is a relatively new area of study. For the study of LFC, a variety of controllers have been suggested, including classical, optimum, adaptive, and robust controllers (Pan CT, Liaw CM (2017)). An adaptive optimum control scheme for AVR is also suggested in a recent publication. As a result of its simplicity and durability, PID controllers are widely used in industries. Only the controller parameters may be tuned. However, the recent development of intelligent methods has addressed this issue.

## 2.0 Materials and Methods

The details of contributions of the present works are as follows. Saadat H (2019):

- (a) For integrated LFC and AVR power systems, the moth flame optimization method is intelligently used.
- (b) This finding examines, from both an LFC and an AVR viewpoint, the importance of various objective functions, including integral of absolute error, integral of time-multiplied absolute error, integral of square error, and integral of time-multiplied squared error.
- (c) An AVR-based excitation voltage control system is used in the first part of this study to illustrate the suggested method for frequency stabilization of isolated power systems.
- (d) PID/FOPID controllers optimized using other intelligent methods are compared to this approach's dynamic response to determining its superiority and efficacy.

(e) Also included in this project are multi-unit two-area power systems. The algorithm's capacity to be tuned is examined in great detail and compared to other algorithms.

AVR-based excitation voltage control is shown in part I, which is devoted to the implementation of the suggested MFO-tuned FOPID control method for frequency stability of isolated power systems. PSO, differential evolution (DE), and GWO-tuned PID controllers are used to evaluate the effectiveness of the suggested approach. A multi-source, multi-area power system with a combined LFC and AVR loop is then added to the current work. Recent publications such as those on ZN- and SA-tuned controllers for the same power system are taken into consideration while analyzing the performance of the MFO-tuned controller suggested.

## 2.1 Load frequency control model

The dynamic model of the LFC loop is described in this section. Generators, turbines, and a speed-regulating framework make up the majority of the power system. The controller input  $\Delta P_{ref}$  and load disturbance  $\Delta P_D$  are the two inputs. These are changes in the generator frequency  $\Delta\omega$  and in the inaccuracy in the area control system (ACE). As a result of Eqs. As follows: (1) and (2) (Wang Y, Zhou R, Wen C (2019)).

$$G_T(s) = \frac{\Delta P_T(s)}{\Delta P_V(s)} = \frac{1}{1 + sT_T} \quad (1)$$

Where  $T_T$  is the turbine time constant,  $\Delta P_T$  is the change in turbine power output and  $\Delta P_V$  is the change in input power to the turbine.

$$G_G(s) = \frac{\Delta P_V(s)}{\Delta P_G(s)} = \frac{1}{1 + sT_G} \quad (2)$$

In this case,  $T_G$  is the governor's time constant, and  $\Delta P_G$  is the governor's power output change over time. Following are some speed load characteristics that may be used to evaluate the spinning mass.

$$\frac{\Delta\omega(s)}{\Delta P_T - \Delta P_D} = \frac{1}{2H + D} \quad (3)$$

H is the inertia constant, and  $\Delta\omega$  is the frequency change. Eq.(4) may be used to correlate the  $\Delta\omega$ , the reference input  $\Delta P_{ref}$ , and  $\Delta P_G$ .

$$\Delta P_G(s) = \Delta P_{ref}(s) - \frac{1}{R} \Delta \omega(s) \quad (4)$$

Where  $R$  is the speed regulation of governor. The frequency biased factor ( $B$ ) is sum of frequency-sensitive load change ( $D$ ) and speed regulation as given below,

$$B = \frac{1}{R} + D \quad (5)$$

## 2.2 AVR system model

As the name implies, an AVR is used to maintain the terminal voltage of an AC generator at a preset level. Sensor, amplifier, exciter, and generator are the four essential components of a simple AVR system. Models for amplifiers, exciters, generators, and sensors are described in Eqs by their input-output relationships. (6), (7), (8) and (9), respectively.

## 2.3 Amplifier model

$$\frac{V_R(s)}{V_e(s)} = \frac{K_a}{1 + T_a s} \quad (6)$$

Tens-to-hundredths of a power amplifier's gain,  $K_a$ , and temporal constant,  $T_a$ , are within reach.

## 2.4 Exciter model

$$\frac{V_F(s)}{V_R(s)} = \frac{K_e}{1 + T_e s} \quad (7)$$

Its gain  $K_e$  is between 10 and 400, and its exciter time constant  $T_e$  is between 0.5 and 1 second.

## 2.5 Generator model

$$\frac{V_t(s)}{V_F(s)} = \frac{K_{field}}{1 + T_{field} s} \quad (8)$$

The gain  $K_{field}$  may range from 0.7 to 1.0, while the time constant  $T_{field}$  can be anywhere from 1.0 to 2.0 s in length.

## 2.6 Sensor model

$$\frac{V_s(s)}{V_t(s)} = \frac{K_S}{1 + T_S s} \quad (9)$$

Time constants  $T_S$  range from 0.001 to 0.06 seconds. The gain  $K_S$  is about 1.0.

## 2.7 Relation of LFC and AVR model

There are three inputs to the generator load system:  $\Delta P_{\text{Real}}(s)$ ,  $\Delta P_T(s)$ , and  $\Delta P_D(s)$ . The generator load system has one output  $\Delta \omega$ , given by, when the AVR model is taken into account (Yamashita K, Taniguchi T (2017)).

$$\Delta \omega(s) = \frac{1}{2Hs + D} [\Delta P_T(s) - \Delta P_D(s) - \Delta P_{\text{Real}}(s)] \quad (10)$$

Where

$$\Delta P_{\text{Real}} = P_s \Delta \delta + K_1 \Delta V_F \quad (11)$$

In addition, the equation may be written as follows to include the minor impact of rotor angle on the generator terminal voltage:

$$\Delta V_t = K_2 \Delta \delta + K_3 \Delta V_F \quad (12)$$

The following is an expression for the modification of the generator field transfer function to incorporate the effects of rotor angle and stator emf:

$$\Delta V_F = \frac{K_{\text{field}}}{1 + sT_{\text{field}}} (\Delta V_e - K_4 \Delta \delta) \quad (13)$$

In this case, the variables  $K_1$ ,  $K_2$ ,  $K_3$ , and  $K_4$  are used. Figures 1 and 2 illustrate a linearized transfer function model for the combined LFC and AVR system.

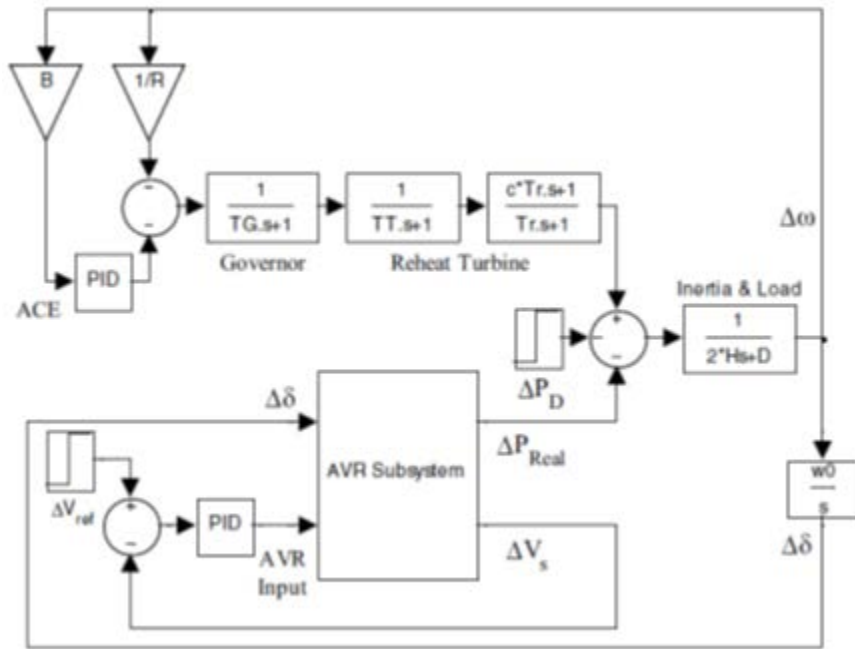


Figure 1: Cordinated LFC and AVR Loop of Isolated Power System

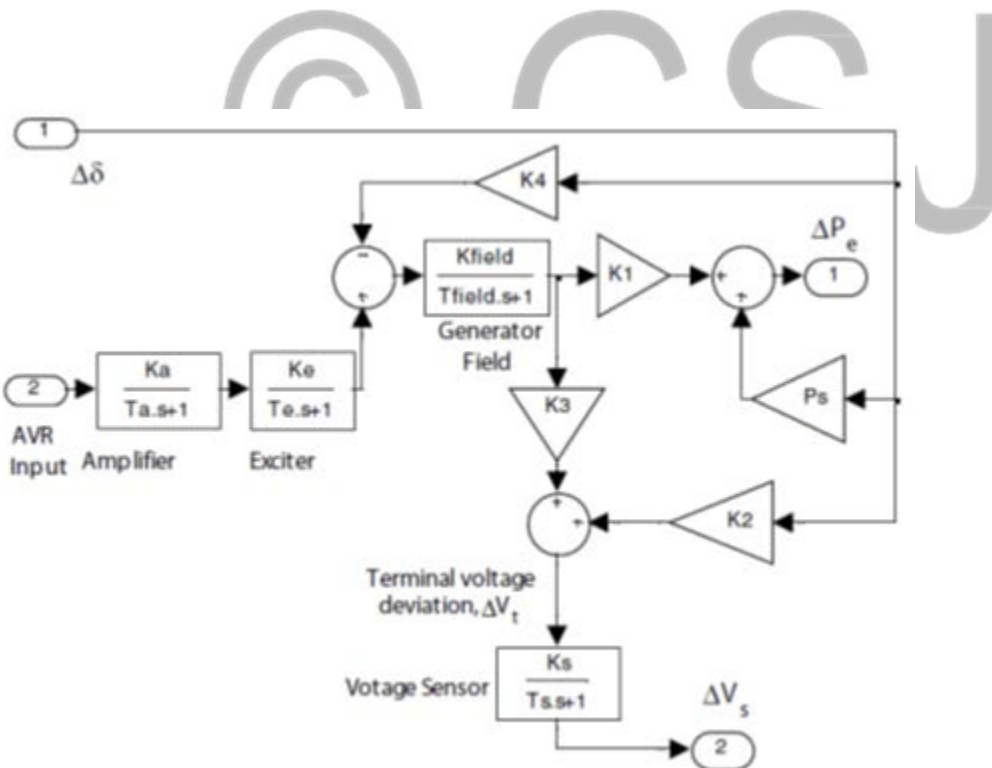


Figure 2: Simulink Model of AVR Sub System

## 2.8 Controller structure and objective function

Most commercially available controllers employ a PID algorithm to enhance dynamic responsiveness while minimizing steady-state inaccuracy. As seen in Equation 14, the PID controller's transfer function is:

$$G_C(s) = K_P + \frac{K_I}{s} + K_D s \tag{14}$$

The controller's gains are  $K_P$ ,  $K_I$ , and  $K_D$ . It is written as follows for a FOPID controller :

$$G_C(s) = K_P + \frac{K_I}{s^\lambda} + K_D s^\mu \tag{15}$$

This is the range of values for, which  $\lambda$  denotes the order of integration, and, which  $\mu$  indicates the order of differentiation PID-order PID controllers provide greater flexibility, but the extra FO controller settings and have a better system dynamic.

If  $\lambda = 1$  and  $\mu = 1$ , the equation may be simplified to a PID controller with integer-order coefficients. Figure 3 shows the FOPID controller's construction. Figure 4 shows the MATLAB/Simulink block for the FOPID controller.

Poles and zeros in FO differ-integers are almost limitless. Band-limited implementations of FO controllers are essential from a practical perspective. However,

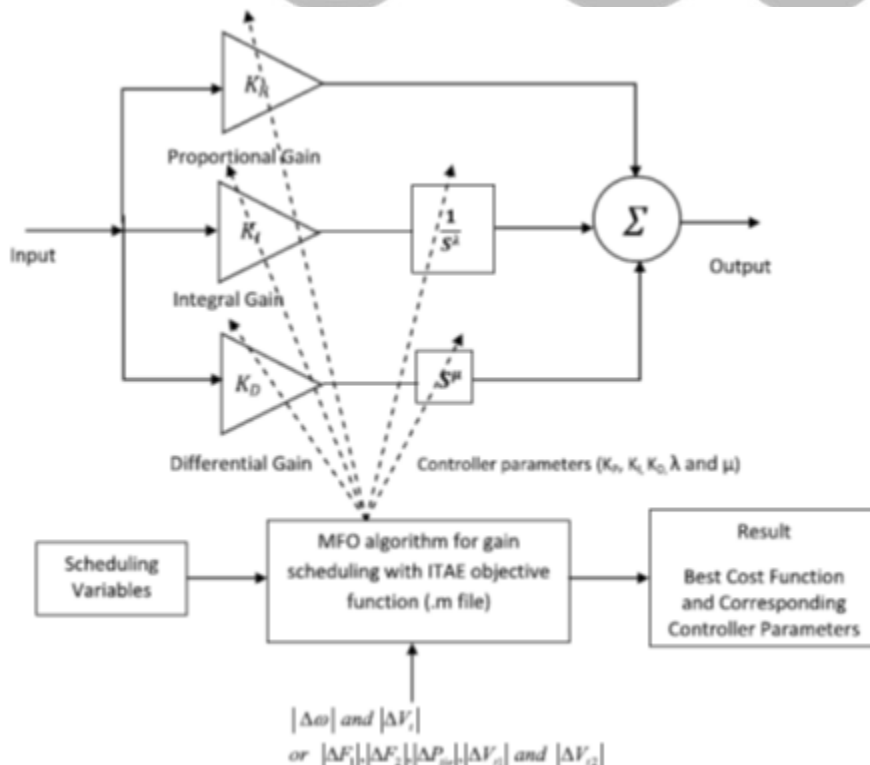


Figure 3: FOPD Controller

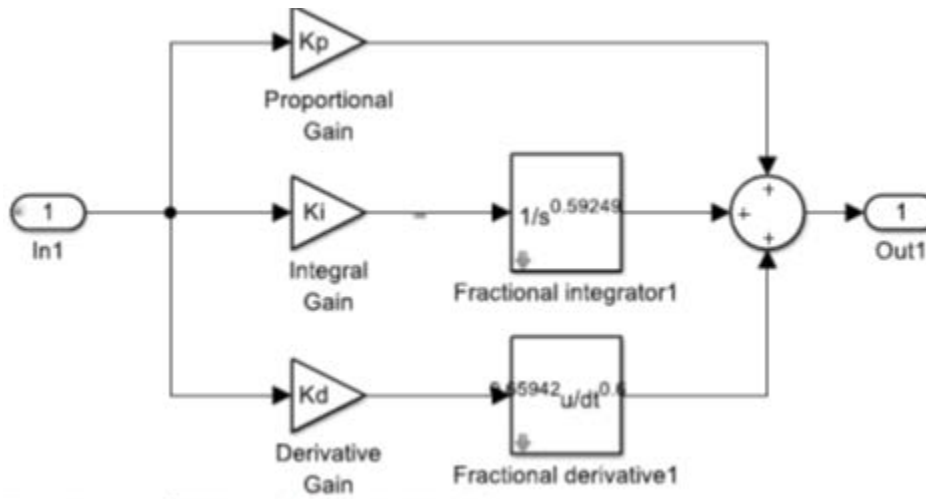


Figure 4: Matlab/Simulink of FOPD Controller

a limited number of poles and zeroes may be achieved by utilizing Oustaloup's CRONE approximation. It is possible to write a higher-order filter with an order of  $(2N + 1)$  that closely approximates FO elements  $s^\alpha$  inside a specified frequency range  $[\omega_L, \omega_H]$ . (16):

$$G_f(s) = s^\alpha \approx K \prod_{k=-N}^N \frac{s + \omega'_k}{s + \omega_k} \quad (16)$$

The order of differentiation and integration is  $\alpha$ , whereas the order of the approximation filter is  $(2N + 1)$ . A recursive formula may be used to get  $K$ ,  $\omega'_k$ ,  $\omega_k$ , and  $k$ .

$$K = \omega_H^\alpha \quad (17)$$

$$\omega'_k = \omega_L \left( \frac{\omega_H}{\omega_L} \right)^{\frac{k+N+\frac{1}{2}(1-\alpha)}{2N+1}} \quad (18)$$

$$\omega_k = \omega_L \left( \frac{\omega_H}{\omega_L} \right)^{\frac{k+N+\frac{1}{2}(1+\alpha)}{2N+1}} \quad (19)$$

An approximation of Oustaloup's fifth order is considered for all FO elements in the frequency range  $\omega \in \{10^{-3}, 10^3\}$  rad/s. It is first determined what the goal function is in terms of desired requirements and limitations.

### 3.0 RESULT AND DISCUSSION

Figures 1 and 2 show the MATLAB/Simulink environment used to construct the system under discussion. LFC and AVR loops are coordinated in a power system that is exposed to a 0.01 per unit step load disturbance. Figure 2 shows the AVR subsystem model. Controller gains for both LFC and AVR loops are maximized utilizing PSO, DE, GWO and MFO. Programs for the algorithms described above are written in (.mfile). This means that the parameters of controllers that have been chosen fall between [0, 2]. Parameters for MFO in this study are population size = 20, maximum iterations = 100. Objective functions IAE, ITAE, ISE, and ITSE are taken into account while determining the optimum weights of the controller. The optimization process is repeated 30 times since intelligent procedures are stochastic in nature. From a total of 30 separate simulations, Table 1 shows the best controller improvements resulting from the least objective function as fitness score. PID controllers are optimized utilizing a variety of techniques in the simulation studies.

**Table 1 Optimum value of controller parameters with different objective function using MFO algorithm for isolated power system (test system 1)**

Controller parameter	IAE	ITAE	ISE	ITSE
LFC loop				
KP	1.998	1.9996	1.9988	1.9989
KI	0.2387	0.0012	0.814	0.4289
KD	1.9994	1.7947	1.9956	1.9967
AVR loop				
KP	0.5934	0.3959	1.9968	1.9996
KI	1.9996	1.9998	1.9942	1.9887

KD	0.2412	0.5461	0.0773	0
----	--------	--------	--------	---

**Table 2 Comparative performance of peak overshoots and settling times (for 2% tolerance band) with different objective function value for isolated power system (test system 1)**

Techniques objective Function	Frequency deviation $\Delta\omega$			Terminal voltage deviation ( $\Delta V_t$ )		
	Maximum overshoot (OS) $\times$ 10 <sup>-4</sup> (p.u.)	Minimum undershoot (US) $\times$ 10 <sup>-4</sup> (p.u.)	Settling time (s) (T S ) for 2% tolerance band	Maximum overshoot (OS) $\times$ 10 <sup>-4</sup> (p.u.)	Minimum undershoot (US) $\times$ 10 <sup>-4</sup> (p.u.)	Settling time (s) (T s ) for 2% tolerance band
MFO PID/IAE	6.6059	- 33.1111	23.077	3.0245	- 0.6085	7.149
MFO PID/ ITAE	2.7904	- 34.2661	21.838	3.3676	- 0.3439	8.28
MFO PID/ISE	13.1665	- 31.1161	38.794	2.5433	-1.0643	7.154
MFO PID/ITSE	9.1126	- 32.2547	31.528	2.7048	- 0.7529	7.692

Italics values are showing the best value in column wise

cost functions. The performance criteria of the framework in terms of peak overshoot, undershoot and settling time are given in Table 2

A and B illustrate the system's frequency and terminal voltage responses. Results indicate that when ITAE is used as an objective function, the minimal settling time can be determined with high accuracy. ITAE is utilized as the goal function, which results in values that are extremely close to ISE when employed as a fitness function. Further analysis will be conducted based on

ITAE. System dynamics may be used to evaluate the MFO technique's execution. Using various methods, Table 2 presents the controller settings and performance indices for peak overshoot, minimum undershoot, settling time (2 percent tolerance range), and ITAE target values.

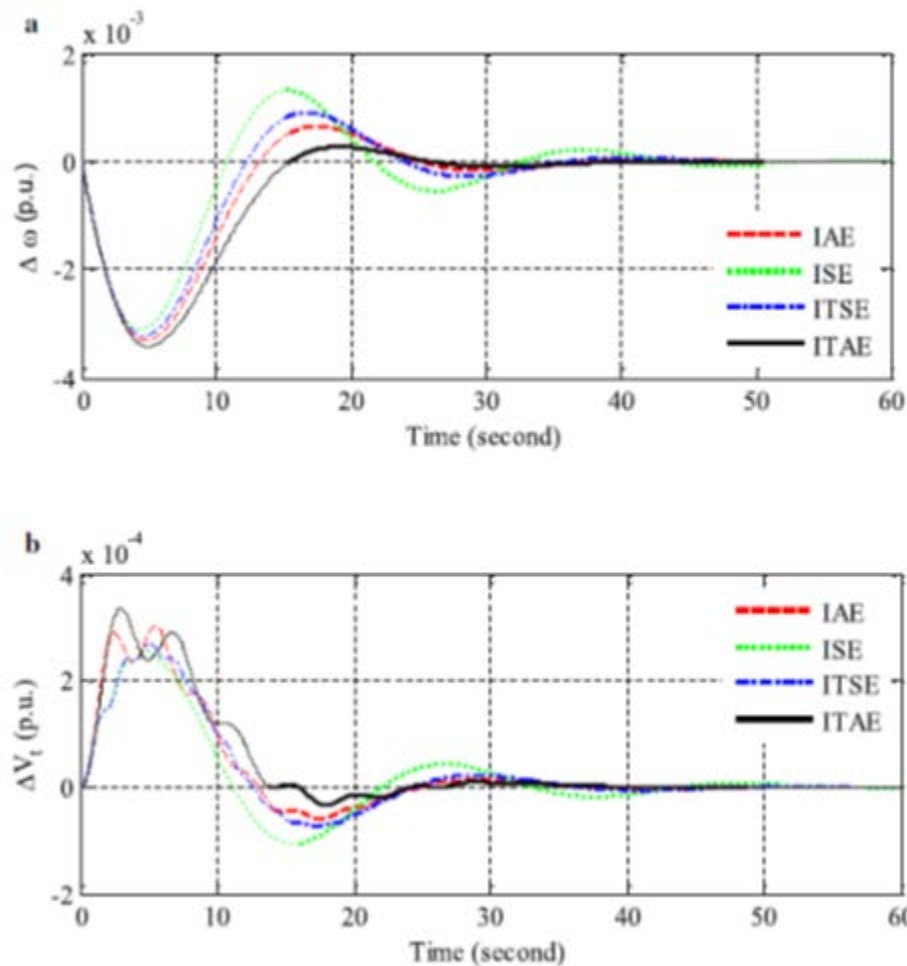


Figure 5: a. Frequency Deviation , b. Terminal Voltage of the System

#### 4.0 Conclusion and Recommendation

An overview and execution study of a PID and FOPID-controlled power system for simultaneous load frequency and automated voltage regulation is presented in this article. The research examines the use of the MFO algorithm, a strong new optimization method inspired by nature, with the aim of addressing the control problem. For optimal global solutions, it's important to highlight that the MFO method only needs a small number of regulating parameters. An AVR-based excitation voltage control system is used in the first portion of the study to illustrate the suggested method for frequency stabilization of isolated power systems. Using

other intelligent methods to optimize PID controllers, the suggested strategy's supremacy and viability are confirmed. Indexes of peak performance

## 5.0 Reference

Beaufays F, Abdel-Magid Y, Widrow B (2019) Application of neural networks to load-frequency control in power systems. *Neural Netw* 7(1):183–194

Elgerd OI (2018) *Electric energy system theory: an introduction*, 2nd edn. McGraw-Hill, New York

Elgerd OI, Fosha C (2019) Optimum megawatt frequency control of multi-area electric energy systems. *IEEE Trans Power Appar Syst PAS-89(4)*:556–563

Fosha CE, Elgerd OI (2019) The megawatt frequency control problem: a new approach via optimal control theory. *IEEE Trans Power Appar Syst PAS-89(4)*:563–577

Ismail A (2020) Robust load frequency control. In: *Proceedings IEEE conference on control applications*, vol 2. New York, Dayton, pp 634–5

Kumar P, Kothari DP (2016) Recent philosophies of automatic generation control strategies in power systems. *IEEE Trans Power Syst* 20(1):346–357

Pan CT, Liaw CM (2017) An adaptive controller for power system load-frequency control. *IEEE Trans Power Syst* 4(1):122–128

Saadat H (2019) *Power system analysis*. McGraw-Hill, New York

Wang Y, Zhou R, Wen C (2019) Robust load-frequency controller design for power systems. *Proc Inst Electr Eng C* 140(1):111–116

Yamashita K, Taniguchi T (2017) Optimal observer design for load frequency control. *Int Electr Power Energy Syst* 8(2):93–100